Beyond Finite-Size Scaling in Solidification Simulations

Frederick H. Streitz, James N. Glosli, and Mehul V. Patel
Lawrence Livermore National Laboratory, Livermore, California 94550, USA
(Received 8 September 2005; published 8 June 2006)

Although computer simulation has played a central role in the study of nucleation and growth since the earliest molecular dynamics simulations almost 50 years ago, confusion surrounding the effect of finite size on such simulations has limited their applicability. Modeling solidification in molten tantalum on the Blue Gene/L computer, we report here on the first atomistic simulation of solidification that verifies independence from finite-size effects during the entire nucleation and growth process, up to the onset of coarsening. We show that finite-size scaling theory explains the observed maximal grain sizes for systems up to about 8 000 000 atoms. For larger simulations, a crossover from finite-size scaling to more physical size-independent behavior is observed.

DOI: 10.1103/PhysRevLett.96.225701 PACS numbers: 64.60.Qb, 64.70.Dv, 81.30.Fb

The nucleation and growth of a solid out of a liquid is a ubiquitous phenomenon that, though well studied, is hardly well understood [1–9]. One of the difficulties associated with this process is the broad range of applicable time and length scales: although the initial nucleation of solidlike regions occurs on the atomic scale, the subsequent rapid growth of these nuclei takes a large fraction of a nanosecond and produces grainlike objects which can involve hundreds of thousands of atoms. The eventual coalescence of these objects results in an interconnected network of grains and grain boundaries which span the entire structures. Computer simulations are a natural way to study this process, but the necessarily finite size of such models is known to color the results. The expectation has always been that a sufficiently large simulation cell would circumvent these issues, producing an accurate model of reality. Researchers have disagreed on exactly how large such a cell must be, with estimates ranging from a few hundred [2] to tens of thousands [5,8].

To address this question, we performed a series of calculations modeling the pressure-induced solidification of tantalum in systems ranging in size from 64 000 atoms (64k) to 32 768 000 atoms (16M) using up to 65 536 processors on the Blue Gene/L computer at LLNL [10]. The complex interatomic interactions were modeled using quantum-based model generalized pseudopential theory, which have been shown to accurately describe the directional bonding in central *d*-electron transition metals at both ambient and under extremes of pressure and temperature [13–15]. An *NVT* ensemble (fixed *Number* of particles, *Volume*, and *Temperature*) was implemented for these simulations, with temperature control provided by application of a Langevin thermostat [16,17]. We used a symplectic integration scheme (with a time step of 1.5 fs) as described by Martyna and co-workers (with a slight modification to incorporate the stochastic thermostat) [18–20].

The initially liquid collection of atoms was isothermally compressed by exponentially decreasing the volume from an initial value of 121.6 a.u. to 74.6 a.u. with a time constant of 100 ps. We show in Fig. 1 the evolution of the solid fraction of the system, as well as the compression. The point marked (*) notes the crossing of the equilibrium melt pressure for this temperature (43 GPa). Nucleation is seen to occur at (a), nearly 100 ps after the equilibrium melt pressure was reached. It is unclear at this time whether the delay represents a true lag for nucleation, or whether the pressure at this time (160 GPa) corresponds to a pseudospinodal for this system (e.g., the point at which solid nucleation can occur with minimal energy barrier) [21,22]. We are currently performing simulations at different strain rates to investigate this further.

Regardless of the nature of the nucleation, rapid growth of the solid grains then occurs (b), with the solidification rate far exceeding the compression rate. This high growth period ends at (c) when the grains have grown into each other (the onset of coalescence). At (c), approximately

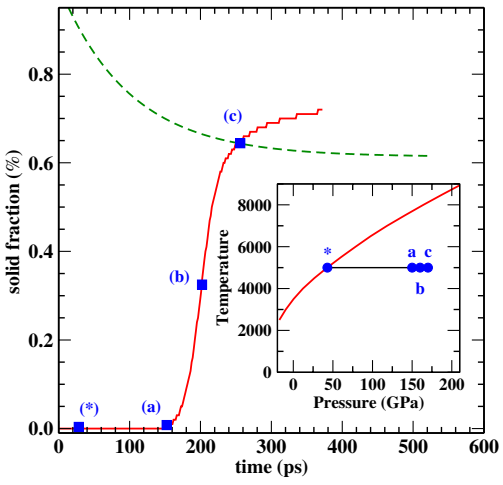

FIG. 1 (color online). Percentage of the simulation cell that has solidified as function of time (solid line), along with the compression ratio (dashed line). The melt curve for Ta is shown in the inset, which also depicts the isothermal compression path (black arrow). The labeled points refer to (*) the crossing of the equilibrium melt curve, (a) the onset of nucleation, (b) the period of explosive growth, and (c) the onset of coalescence.

65% of the material has solidified—the remaining material comprises an extensive, percolating network of liquid and disorder separating grains of differing orientation [23]. The percolation threshold is reached from above, as liquid is consumed by the growing solid. From this point forward. the continued growth of grains is no longer accomplished by the speedy conversion of free liquid atoms but rather by the assimilation of smaller grains by larger grains—a far slower process mediated by the network of disorder which spans the simulation cell [24].

We display in Figs. 2(a)–2(c) a time sequence of cross-sectional images obtained from slices of a 16M-atom simulation cell at the points marked (a)–(c) in Fig. 1. In Figs. 2(d)–2(f) we show the same sequence for a 64k-atom simulation. The atoms have been colored according to a parameter that is a measure of the correlation of local symmetry—liquidlike (blue) atoms have local symmetry which is poorly correlated, while solid (red) atoms posses a local symmetry which is highly correlated with their neighbors [25]. Yellow atoms identify a distinct population of ''intermediate'' atoms that occupy the interfaces and grain boundaries. The images for the 64k-atom simulation were created by tiling the original slices (using periodic boundary conditions) so that the spatial extent for each of the images approximately matches that of the 16M-atom images. (The images are 6×6 tiles of the original; the exact ratio of simulation box lengths is 6.35:1). Homogenous nucleation in the larger sample is seen to occur earlier and across the entire sample. Nucleation continues to occur as the existing grains grow, producing a heirarchy of nucleus-nucleus separations and sizes that lead to the rich grain structure seen in Fig. 2(c). By contrast, the early grains in the 64k-atoms simulation are almost all nucleated simultaneously. They grow very rapidly to fill the simulation cell, allowing no time for continued nucleation to occur in the spaces [26]. Coalescence in this system produces a very artificial final grain structure, dominated by grains which now span the entire structure. The unphysical nature of this model is discouraging, given the already substantial size of this simulation. The simulation performed with 256k atoms resulted in a grain structure very similar to the patterned structure shown in Fig. 2(f), with grains which span the simulation cell. Interestingly enough, a similar investigation of the structure at coalescence for the 2M

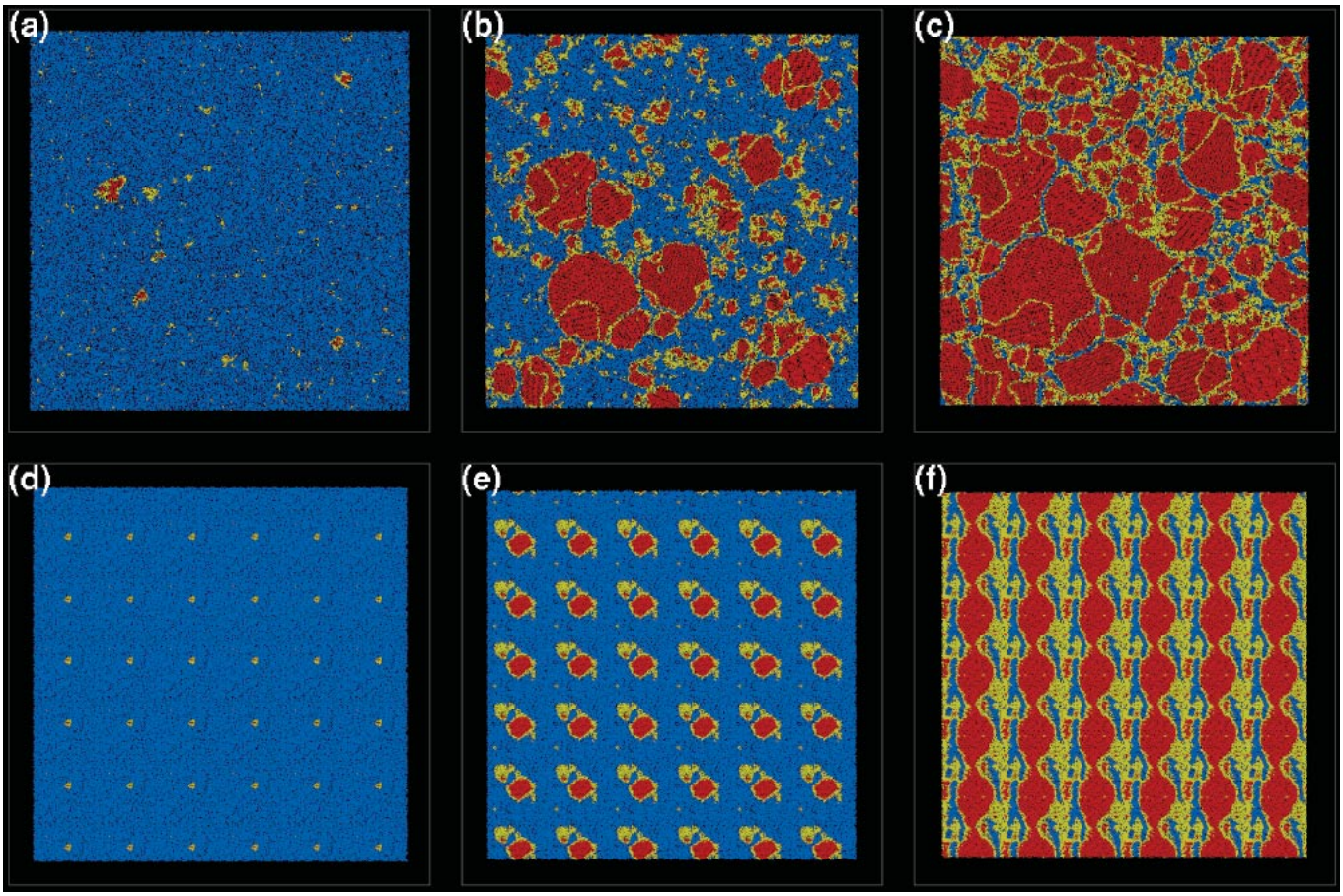

FIG. 2 (color). Cross sections of the 16M-atom (a)–(c) and 64k-atom (d)–(f) simulation taken at different stages during the solidification. Labels (a)–(c) refer to points shown in Fig. 1, while labels (d)–(f) refer to corresponding times for the 64k-atom sample. [Animation of the solidification is available online [26].]

atom simulation did not reveal system-spanning grains—the structure appears (to the eye, at least) similar to that shown in Fig. 2(c), for the 16M atom simulation. A more careful investigation reveals that even in the absence of such a clear "periodic boundary effect," the distribution of grain sizes in this system has also been cut off at an artificially small size. We display in Fig. 3 the average size of the largest grains as a function of time for sample sizes spanning over two orders of magnitude. Although the grains evolve in similar fashion (i.e., explosive growth followed by a slow coarsening after coalescence), the size of the largest grains at the percolation threshold (as the system transitions from fast to slow growth) exhibits a strong size dependence, with the smaller samples unable to attain the larger grain sizes [27]. The dependence of grain size to system size can be described using finite-size scaling theory—close to the percolation threshold, the total number of atoms (or mass, M) in the largest grains should scale as the linear size of the system L with a fractal dimension d_f

$$M \propto L^{d_f}, \qquad d_f = d - \beta/\nu,$$

where the critical exponents are known to be $\beta = 0.41$ and $\nu = 0.88$ for $d = 3$ dimensions. Since the total size of the simulation cell is just $N = L^d$, we expect that in 3 dimensions,

$$M \propto N^{d_f/d} \approx kN^{0.84}.$$

We plot the size at percolation (the points marked in Fig. 3) against simulation-cell size in Fig. 4, as well as the results expected from finite-size scaling (solid line). (The power-law scaling is highlighted in the inset.) We find that for samples smaller than 8 192 000 (8M) atoms, the results can be closely described using finite-size scaling, so that the finite size of the simulation cell is determining the size of the largest clusters. Simulations utilizing cells larger than 8M atoms would not produce larger grains at the percolation threshold, as evidenced by the behavior of the 16 364 000 (16M) and 32 768 000 (32M) atom simulations. For these simulations, continuous nucleation of solid (in the vanishing liquid spaces) and growth of the existing solid grains ultimately serve to limit the grain size. The growth of the largest grains for the 16M atom cell is seen in Fig. 3 to follow almost identically the growth observed in the 8M-atom simulation, while the size of the largest grains at percolation are seen to have significantly departed from the finite-size scaling prediction. We performed a similar simulation on a 1M-atom cell using an NPT ensemble which applies a time-varying hydrostatic stress in contrast to the NVT simulations that directly control the volume. We saw little difference in the growth behavior while using this compression technique to follow substantially the same thermodynamic path—as shown in Fig. 4. The size scale for solidification is thus not influenced by the simulation details. We expect that in general, it is the competition between nucleation and growth that affects the characteristic size at percolation—any solidification process which leaves these two rates unchanged would result in similar scaling behavior [28].

We present the results of very large-scale atomistic simulations of pressure-induced solidification of molten metals performed on the Blue Gene/L computer at LLNL. Using many-body, angular-dependent model generalized pseudopotential theory interaction potentials, we simulated the rapid solidification of tantalum in systems ranging in size from 64 000 atoms to 32M atoms using as many as 65 576 processors. Our calculations, the largest

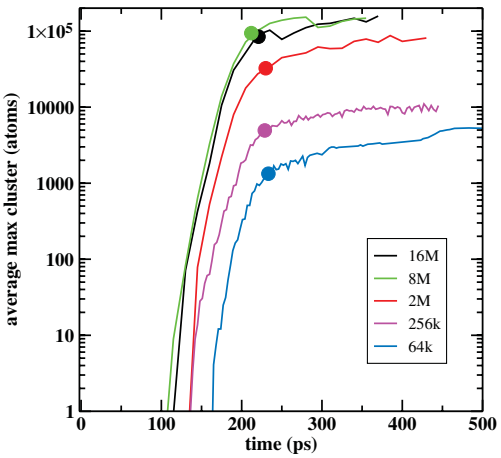

FIG. 3 (color). The average size of the largest clusters in the system as a function of time, plotted for simulation cells containing 64 000 (blue), 250k (magenta), 2M (red), 8M (green), and 16M (black) atoms. The marked points represent the average size of the largest clusters at the onset of coalescence.

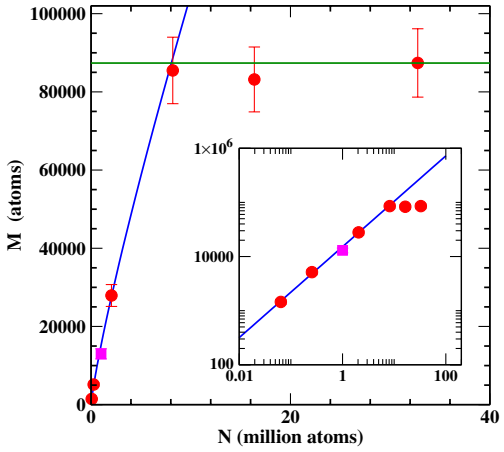

FIG. 4 (color online). Average maximum cluster size at the start of coarsening as a function of simulation size. The solid line represents the result of finite-size scaling theory. We find that the maximum cluster size is independent of system size for simulations larger than about 8M atoms. Inset: log-log plot of the results, showing the linear (power-law) dependence. The 1M-atom simulation (square) was run in an NPT ensemble.

ever attempted with these highly accurate, computationally expensive potentials, demonstrate that modeling solidification with more than 8×10^6 atoms is required to produce initial solidification geometries which are entirely independent of simulation-cell size, a result which does not depend on the details of the simulation.

The authors would like to acknowledge the many dedicated individuals at LLNL and IBM who made Blue Gene/L a functioning reality, and to thank Liam Krauss for valuable assistance in visualizing our data. F. H. S. acknowledges many helpful discussions with Roger Minich. This work performed under the auspices of the U.S. Department of Energy by University of California Lawrence Livermore National Laboratory under Contract No. W-7405-Eng-48.

[1] B. J. Alder and T. E. Wainwright, J. Chem. Phys. **31**, 459 (1959).
[2] M. J. Mandell, J. P. McTague, and A. Rahman, J. Chem. Phys. **64**, 3699 (1976).
[3] J. D. Honeycutt and H. C. Andersen, Chem. Phys. Lett. **108**, 535 (1984).
[4] J. D. Honeycutt and H. C. Andersen, J. Phys. Chem. **90**, 1585 (1986).
[5] W. C. Swope and H. C. Andersen, Phys. Rev. B **41**, 7042 (1990).
[6] M. S. Watanabe, Phys. Rev. E **51**, 3945 (1995).
[7] S.-F. Tsay and I. F. Liu, Phys. Lett. A **192**, 374 (1994).
[8] B. O'Malley and I. Snook, Phys. Rev. Lett. **90**, 085702 (2003).
[9] J. N. Cape *et al.*, J. Chem. Phys. **75**, 2366 (1981).
[10] Blue Gene/L (BG/L), is a massively parallel scientific computing system developed by IBM in partnership with the Advanced Simulation and Computing program (ASC) of the US Department of Energy's National Nuclear Security Agency [11,12]. The 32 768-node system at LLNL is at this writing the fastest computer in the world.
[11] A. Gara *et al.*, IBM J. Res. Dev. **49**, 195 (2005).
[12] S. Chatterjee *et al.*, IBM J. Res. Dev. **49**, 377 (2005).
[13] J. A. Moriarty, Phys. Rev. B **49**, 12 431 (1994); **42**, 1609 (1990).
[14] J. A. Moriarty *et al.*, J. Phys. Condens. Matter **14**, 2825 (2002).
[15] J. A. Moriarty (to be published).
[16] D. L. Ermak and H. Buckholz, J. Comput. Phys. **35**, 169 (1980).
[17] M. P. Allen and D. J. Tildesley, *Computer Simulation of Liquids* (Clarendon, Oxford, 1987).
[18] M. Tuckerman, G. J. Martyna, and B. J. Berne, J. Chem. Phys. **97**, 1990 (1992).
[19] G. Martyna, D. J. Tobias, and M. L. Klein, J. Chem. Phys. **101**, 4177 (1994).
[20] G. J. Martyna *et al.*, Mol. Phys. **87**, 1117 (1996).
[21] W. Klein and F. Leyvraz, Phys. Rev. Lett. **57**, 2845 (1986).
[22] S.-N. Luo, A. Strachan, and D. C. Swift, J. Chem. Phys. **120**, 11 640 (2004).
[23] The critical percolation probability for random percolation in three dimensions is about 31%.
[24] D. Stauffer, Phys. Rep. **54**, 1 (1979).
[25] P. R. tenWolde, M. J. Ruiz-Montero, and D. Frenkel, Phys. Rev. Lett. **75**, 2714 (1995).
[26] See EPAPS Document No. E-PRLTAO-96-045622 for an animation sequence of the two nucleation events. For more information on EPAPS, see http://www.aip.org/pubservs/epaps.html.
[27] Both the rapid initial growth rate and the slow (coarsening) growth rate appear to be independent of size.
[28] J. N. Glosli and F. H. Streitz (to be published).